# Thermal radiation anomalies associated with major earthquakes

Dimitar Ouzounov[1], Sergey Pulinets[2], Menas C. Kafatos[1] and Patrick Taylor[3]

[1] Chapman University, CEESMO, Orange, CA, USA.

[2] Space Research Institute, RAS, Moscow, Russia.

[3] NASA GSFC, Greenbelt, MD, USA.

Corresponding author: Dimitar Ouzounov (Ouzounov@chapman.edu)

**Key Points:**

- ☐ Identify a method of recognition for pre-earthquake thermal radiation anomalies.

- ☐ Estimate of thermal energies associated with some large earthquakes.

- ☐ Described a mechanism for pre-earthquake thermal radiation anomalies generation.

**Abstract**

Recent developments of remote sensing methods for Earth satellite data analysis contribute to our understanding of earthquake related thermal anomalies. It was realized that the thermal heat fluxes over areas of earthquake preparation is a result of air ionization by radon (and other gases) and consequent water vapor condensation on newly formed ions. Latent heat (LH) is released as a result of this process and leads to the formation of local thermal radiation anomalies (TRA) known as OLR (outgoing Longwave radiation, Ouzounov et al, 2007). We compare the LH energy, obtained by integrating surface latent heat flux (SLHF) over the area and time with released energies associated with these events. Extended studies of the TRA using the data from the most recent major earthquakes allowed establishing the main morphological features. It was also established that the TRA are the part of more complex chain of the short-term pre-earthquake generation, which is explained within the framework of a lithosphere-atmosphere coupling processes.

List of Acronyms:
AVHHR- Advanced Very High Resolution Radiometer( NOAA)
ACP- Atmospheric chemical potential
EMSC- European-Mediterranean Seismological Centre
EOS - Earth Observation System (NASA)
AIRS –Atmospheric Infrared Sounder (NASA)
EQ-earthquake
GMSD –IGS GPS station in Japan
GOES - Geostationary Operational Environmental Satellite (NOAA)
ISTF- Integrated satellite and terrestrial framework
LAIC- Lithosphere-Atmosphere-Ionosphere Coupling
LH – Latent heat
LWR – Long wave radiation
LAIMC - Lithosphere-Atmosphere-Ionosphere-Magnetosphere Coupling
POES - Polar Operational Environmental Satellites  (NOAA)
OLR –Outgoing Longwave Radiation
RST- Robust Satellite technique
STIR- Satellite thermal infrared radiation
SW –short wave radiation
TIR-Thermal Infrared radiation
TOA – Top of the Atmosphere
USGS-US Geological Survey

# 1. Introduction

The search for physically based pre-seismic signals has been conducted for many years (e.g., Martinelli, 1998). Multiple observations of earthquake precursory signals have previously been published (Hayakawa M, (Ed), 1999, Hayakawa M. and O.A.Molchanov (Ed), 2002, Pulinets and Boyarchuk, 2004). Recent analyses of data from multi-instrument space-borne and ground observations have provided evidence for the existence of pre-earthquake atmospheric signals (Han et al, 2014, 2016, Hayakawa (Ed)  2012, Kon et al, 2010 , Liu et al 2000, 2010,  Tramutoli et al, 2015a,b,, Ouzounov et al, 2011 , Pulinets and Davidenko, 2014) These studies have contributed to our understanding of the physics of earthquakes and the phenomena that precede their energy release. Recent advances in earth observing space technology have also helped to advance the scientific understanding of the nature of pre-earthquake phenomena in the atmosphere. We are searching for pre-seismic observations that might give warning of a major earthquake. Our investigation is

based on a search for possible connection between satellite observations (latest NPOESS - National Polar-orbiting Operational Environmental Satellite System and NASA EOS - Earth Observing System) of anomalous atmospheric thermal transient signals and subsequent major earthquakes.
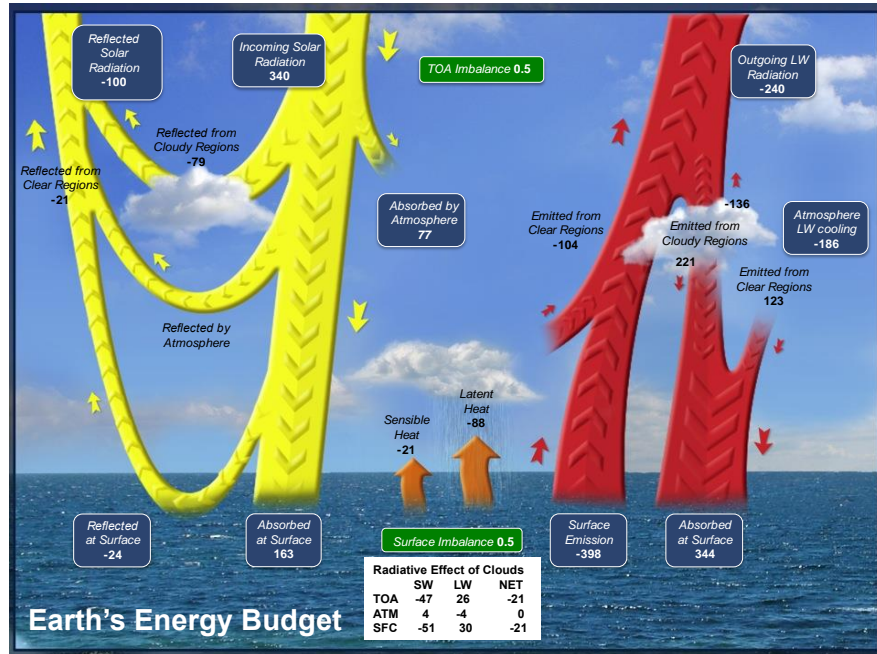


*Fig. 1. Earth Atmospheric Energies, (*Earthobservatory.nasa.gov*, NASA, 2012)*

Figure 1, the Earth's Energy Budget (Earthobservatory.nasa.gov), shows that more than 70% of the reflected solar radiation occurs in the atmosphere. While the Earth surface absorbs incident shortwave (SW) solar energy nearly one third is reflected back into space. The heat absorbed at the surface does not reach any significant depth because the surfaces low thermal conductivity. The absorbed energy instead is re-emitted as long wavelength radiation (LWR) energy mostly during the nighttime.

The energy directly released into the atmosphere, is known as sensible heat (SH)- and is transferred as radiant thermal energy or heat. This latent heat (LH) is the energy released or absorbed by a substance during a phase change. A balance must exist between incoming and radiated solar energy or else the surface of Earth would permanently heat up. This process of radiative exchange is complex. Generally the LWR emitted by the Earth into the atmosphere gets absorbed and maintains a thermal equilibrium with the atmosphere. When the sky is clear the LWR escapes into space since the atmosphere is "transparent" to the radiation in the 8.0-12.0 μm spectral wavelengths. Sometimes this atmospheric window can be partially blocked by clouds or pollution and outgoing LWR could be reabsorbed by the atmosphere and re-emitted in all directions.

The outgoing LWR at the top of the atmosphere (TOA) has been estimated by satellite sensors as outgoing long wave radiation (OLR). The net result is that radiative losses from the atmosphere are generally balanced by the energy re-emitted as heat from Earth's surface. Later, mainly during the formation of clouds, the water vapor condensates and the LH is released into the atmosphere (estimated by SLHF from NCEP). This leads to heat transfer from the surface into the atmosphere, which is one of the main drivers of the general, atmospheric circulation (Goosse et al, 2016)

**2.Methods for recognition of thermal radiation anomalies (TRA)**

For more than 2000 years scientists have been searching for signals preceding earthquakes. According to ancient Greek philosopher Aristotle, "pneuma" (wind/gas) are involves before earthquakes producing strange atmospheric effects (MacArthur, 1980). The fundamental meaning of "pneuma" is air in motion or electricity in the airs. Fogs and

clouds were recognized as observational evidence for activities prior to major seismicity since the days of Aristotle and Pliny (Roman Empire) and many researchers in ancient China (Tributsch, 1978). John Milne - an English seismologist and geologist who invented the first modern seismograph has published the first quantitative analysis of atmospheric signals associated with seismicity (Milne, 1913). He found that for 387 earthquakes in Northern Japan, the sinuses of the curves of means monthly temperature were generally a little ahead of the crest of the waves indicating the earthquake arrival (Milne, 1913).

Just recently a comprehensive catalog of atmospheric pre earthquake signals based on historical and instrumental record for more than 1500 earthquakes between 550 BA until 2000AD been published (Tronin, 2011). Several atmospheric parameters  (atmospheric heat, drought, cooling, clouds, air pressure variations, winds, fogs, etc.) have been found before the seismic shocks occurrence related to about 700 earthquakes ( ~50%  from the all cases ) and  only temperature increased been seen in 10% of the cases , which is still  a good indicator, having in mind the thermometer been invented only in 16$^{th}$ century. In addition to the atmospheric phenomena variety of hydrological changes been reported usually followed by gas release (bad smell) and fogy atmosphere (Tronin, 2011).

The recent advances in remote sensing   instruments have helped to advance the scientific understanding of atmospheric earthquake signals. Satellite thermal imaging data reveal stationary (long-lived) thermal anomalies associated with large linear structures and fault systems in the Earth's crust (Carreno et al., 2001) but also transient (short-lived) anomalies prior to major earthquakes (Quing et al., 1991, Salman et al., 1992). Their spatial extent and temporal evolution may be dependent on local geology and tectonics, nature of the focal mechanism, meteorological conditions and other factors. Studies on the relationship between satellite thermal infrared (TIR) data and earthquake precursors have been based on data from both single and multi-instruments . Gorny et al. (1988), Tronin et al. (2002,2004),  Dey et al. (2004), Saraf et al, (2005) have used imagery recorded by Advanced  very-high-resolution radiometer (AVHRR), analysis methods based on a comparisons between before and after images over an an earthquake epicenter. Newer techniques have been proposed, using sub-pixel level co-registration and geo-referenced data from both polar-orbiting and geosynchronous satellites (GOES, Meteosat, AVHRR, and Landsat (Bryant et al., 2003; Di Bello et al., 2004).One of the problems in detecting TIR anomalies  is defining abnormal TIR fluctuations from a normal baseline. To address this problem, an approach was developed using a time series of TIR data over earthquake prone regions. Using pixel-level thermal radiation variance from established base lines, it was possible to identify anomalous TIR signals (Tramutoli et al., 2001, Filizzola et al., 2004, Cervone et al., 2006, Ouzounov et al, 2007). After the launch of the EOS satellites (1999-Terra and 2002-Aqua), a new approach for detecting pre-earthquake anomalies was developed, based on Land Surface Temperature (LST) derived from the 11-micron data (Ouzounov and Freund, 2004). Observations with NPOESS and the EOS Aqua's Atmospheric Infrared Sounder (AIRS) of atmospheric environmental parameters have revealed an increase in radiation and a transitional change in Outgoing Longwave Radiation (OLR) in the 8-12 micron range (Ouzounov et al., 2007). OLR transitional changes recorded at the TOA (top of the atmosphere) over seismically active regions have been proposed as being related to thermodynamic processes within the earth's crust that lead to earthquakes (Ouzounov et al., 2011; Pulinets and Ouzounov, 2011).

## 2.1 Robust Satellite technique
Space–time anomalies of Earth's emitted radiation in the thermal infrared spectral range (TIR) measured from satellite months to weeks before an earthquakes, have been interpreted, by several authors, as pre-earthquake signals (Qiang et al., 1991; Tronin , 1996,2006; Gorny et al. 1988;Tramutoli et al., 2005).
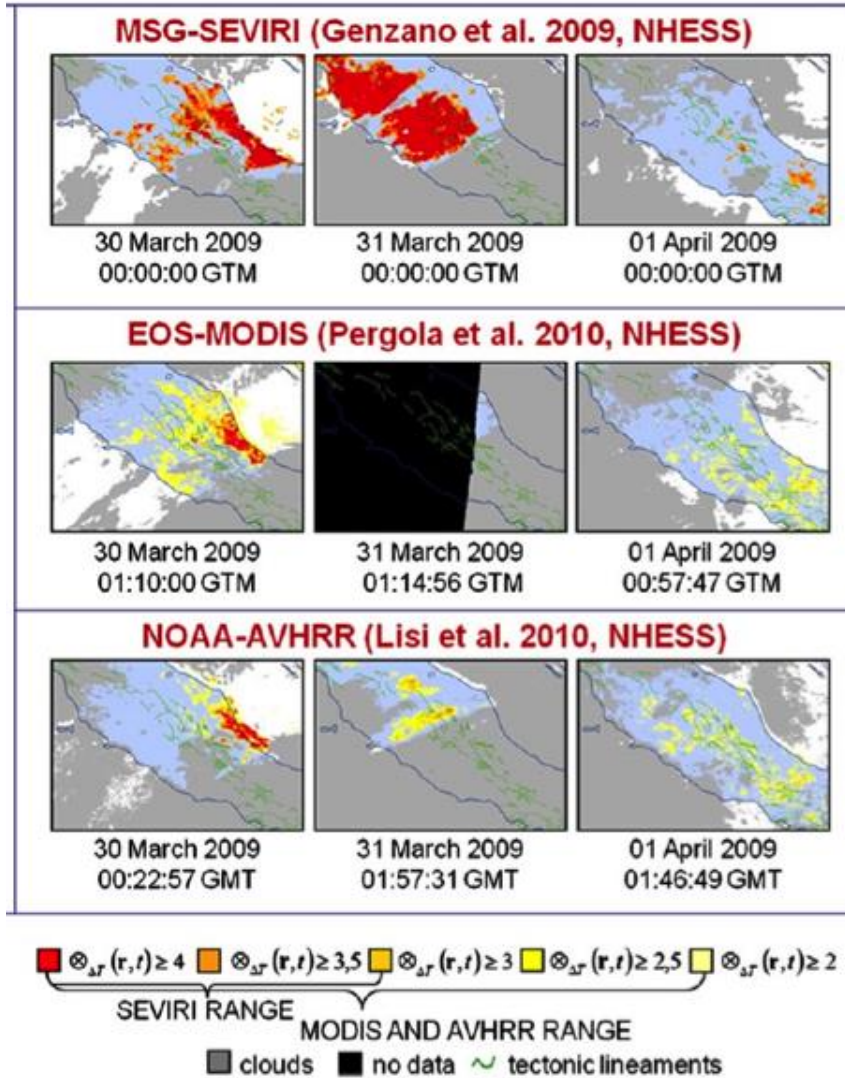
*Fig.2 RST application for seismically active areas show space-time correlation between thermal anomalies and earthquakes occurrence. The case of L'Aquila earthquake (6 April 2009, $M_w$ 6.3) by using (top to bottom) both polar (Lisi et al., 2010; Pergola et al., 2010 for NOAA/AVHRR and EOS/MODIS) and geostationary (MSG/SEVIRI, Genzano et al., 2009) sensors respectively.*

The claimed connection of TIR emission with seismic activity has been considered, for a long time with some caution, by the scientific community mainly because of the insufficiency of validated data-sets and the scarce importance attached by those authors to other causes (e.g. meteorological) that, rather than seismic activity, could be responsible for the observed TIR signal fluctuations (for a review see Tramutoli et al., 2015a,b and reference herein). The Robust Satellite technique (RST) technique is based on a preliminary multi-temporal analysis on several years of homogeneous historical dataset of satellite TIR records, which are devoted to interpreting the TIR signal for each pixel of the satellite observations. Anomalous TIR patterns are identified using a specific index, RETIRA (Robust Estimator of TIR Anomalies, Filizzola et al., 2004; Tramutoli, 2005). Quality of TIR data analyses and of the validation processes devoted to assess the possible correlation among TIR anomalies and seismic activity have been improved in recent years (Tramutoli et al., 2015b), increasing the possibility of including them among the observables which are expected to positively contribute to an advanced multi-parametric system for a time-Dependent Assessment of Seismic Hazard (Elefteriou et al., 2015, Tramutoli et al., 2014a, 2014b). In particular, the Robust Satellite data analysis Technique (RST) proposed in 1998 by Tramutoli (see also Genzano et al, 2007) has been successfully

applied in order to identify pre-earthquake space–time TIR anomalies even in very variable observational (satellite view angle, land topography and coverage, etc.) and normal (e.g. meteorological) conditions. In subsequent RST applications to different seismically active areas, the space-time correlation between thermal anomalies and earthquakes occurrence was confirmed. For instance by using both polar (Lisi *et al*., 2010; Pergola *et al*., 2010 for NOAA/AVHRR and EOS/MODIS respectively) and geostationary (MSG/SEVIRI, Genzano et al., 2009) sensors, in the case of L'Aquila earthquake (6 April 2009, $M_w$ 6.3). (See Fig.2)

## 2.2 Outgoing long wave radiation analysis

One of the main parameters used to characterize the Earth's radiation environment is outgoing long-wave-earth radiation (Liebmann and Smith, 1996). OLR has been associated with the top of the atmosphere integrating the emissions from the ground, lower atmosphere and clouds (Ohring G. and Gruber, 1982) and primarily was used to study Earth radiative budget and climate studies (Gruber and Krueger, 1984). Daily OLR data were used to study the OLR variability in the zone of earthquake activity (Liu and Kang 1999; Ouzounov et al., 2007, 2011; Xiong at al., 2010). An increase in radiation and a transient change in OLR was proposed to be related to thermodynamic processes in the atmosphere over seismically active regions and described as thermal radiation anomaly (TRA). Because of today varieties in OLR type of algorithms and data products such as: RBUD – NOAA/CLASS; CERES LWR – TOA fluxes; NOAA/AVHRR –OLR, and EOS Aqua -CLROLR fluxes; we introduce the thermal radiation anomaly (TRA ) as a common name for type of anomalies based on different data for computing the transitional LWR. The anomalous characteristic of TRA was suggested by Ouzounov et al., (2007) as a statistical maximum change in the rate of OLR for a specific spatial location and predefined times and was constructed corresponding to the anomalous thermal field (Tramutoli et al., 1999, 2013). The anomaly represents the different amplitude for a specific spatial location and predefined times:

$$\text{Anomaly}(x, y, t) = \frac{S(x,y,t) - \bar{S}(x,y,t)}{\tau(x,y,t)} \tag{1}$$

$$\bar{S}(x, y, t) = \frac{1}{N}\sum_{i=1}^{N} S(x_i, y_i, t_i) \tag{2}$$

$$\tau(x,y,z) = \sqrt{\frac{\sum\left(S(x,y,t) - \bar{s}(x,y,t)\right)^2}{N}} \tag{3}$$

Where: $S(x, y, t)$ the current OLR value, $\bar{S}(x, y, t)$ the computed mean of the background field, defined as the daily y mean value of OLR $S(x_i, y_i, t_j)$ over an area of longitude *x* and latitude *y* in the $t^{th}$ day of the *M* years and $\tau(x,y,z)$ the standard deviation over the same location(*x,y*) and local time(*t*) as OLR value. This rapid enhancement of radiation could be explained by an anomalous flux of the latent heat over the area of increased tectonic activity. The input data been processed in the native resolution of (2.5x2.5) and the output maps been processed in two steps procedure.: 1/Grid resolution enhancement ( 1x1 degree ) with additional pre-processing for avoiding aliasing of short wavelengths; and 2/ Re gridding with spatial filtering and grid points re computing based on "minimum curvature" algorithm used by standard computation packages (Fisher at al, 2008). In our studies, we used OLR data from NCEP/NOAA's Advance Radiation Radiometer (AVHRR). A daily mean global data base, with a spatial resolution of 2.5º by 2.5º, was used to study the OLR activity and variability in the region of three recent major earthquakes: i/ M7.1 on October 24, 2011 in Van, Turkey; ii/ M6.9 on May 24, 2014 Aegean Sea, Greece and iii/ M6.0 on August 24, 2014 in Napa, CA (See Table 1)

Table 1. List of studied earthquakes (USGS)

| | Name | Date (mm/dd/yyyy) | Geographic lat/lon (°) | Time (UTC) | M | $H$ (km) | |
|---|---|---|---|---|---|---|---|
| 1 | Van, Turkey | 10/25/2011 | 38.62 N/43.48 E | 16:41:00 | 7.2 | 7.1 | |
| 2 | Aegean Sea, Greece | 05/24//2014 | 40.3 N/25.45 E | 09:25:00 | 6.9 | 10 | |
| 3 | NapaValley, California,US | 08/24/2014 | 38.21 N/122.31W | 10:24:44 | 6.0 | 11.11 | |

Our method includes recording the OLR at the top of the atmosphere several days before the onset of an earthquake and characterizes the state of the atmosphere before the earthquake by the established baseline. Calculated at the TOA, OLR from NOAA POES were used to study the Earth's radiation budget, because they represent emissions from the Earth's surface, lower atmosphere, and clouds, and they are sensitive to near surface and cloud temperatures. Observations from the NOAA POES were based on the long-wave flux estimation of Ellingson et al. (1989). Daily mean OLR values were calculated from these raw data, using algorithms based on Eqs. (1-3) and customized for each region. The NOAA Climate Prediction Center (http://www.cdc.noaa.gov/) provides daily and monthly OLR data and the OLR algorithm for analyzing the advanced very high-resolution radiometer (AVHRR) data. A daily mean, covering a significant area of the Earth (90 ° N– 90 ° S, 0 ° to 357.5 ° E) and with a spatial resolution of 2.5 ° x 2.5° recorded.

The "daily values", "normal state" and "TRA anomalies" in relation to pre-earthquake OLR signals were introduced initially by Ouzounov et al., 2007 and Xiong et al. 2010. The "TRA anomaly" has been calculated as a deviation of daily values from the normal state and normalized by the multiyear standard deviation for the same pixel (Eq.1) and shown on Fig.3, 4, and 5 in red. The "Daily values" are daily raw values of OLR for the same pixel and same local time observed by the polar orbit satellite Figs. 3,4, and 5 (gray curve line). The "normal state" for OLR was estimated by a multiyear average (from 2004 to the present) for each pixel (Eq.2) and Figs.3,4, and 5 (black solid curve). The OLR "anomalies" represent the maximum change in the daily variations of the OLR in comparison to the "normal state".

The continuous satellite monitoring of OLR data over Turkey, shows a rapid increase of emitted radiation during mid the September- October 2011 time frame (Fig. 3).An anomaly at TOA was detected at 19:00 LT on October 19, 2011, south east of the epicenter area. The anomaly was spatially extended and temporally persistent for 8 hours and was the largest TRA anomaly over the entire European continent at that time (Ouzounov et al., 2014).
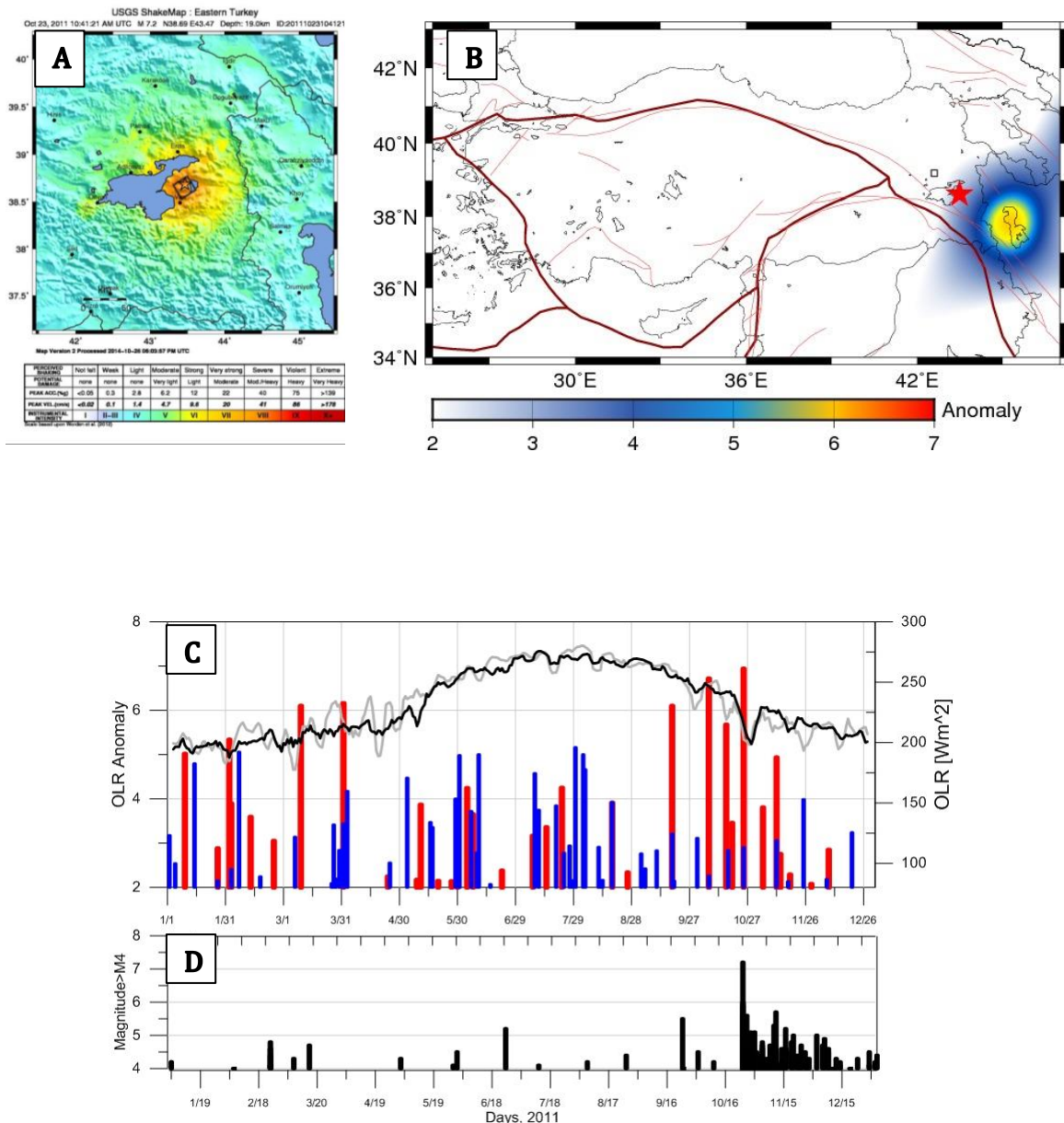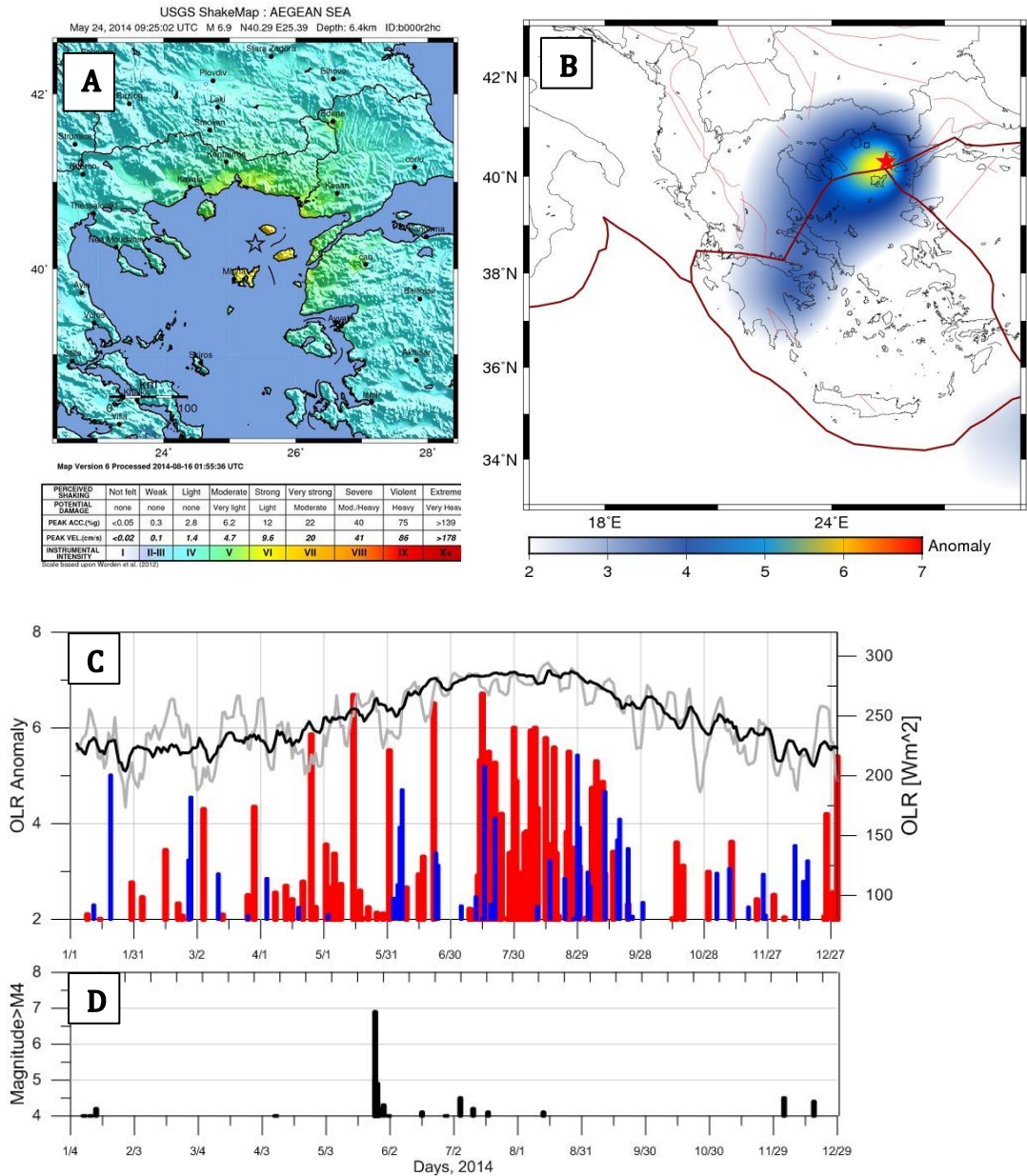
*Figure 3. TRA associated with M7.3 of Oct 23, 2011, Van, Turkey; A/.USGS shake map (top left), B. Nighttime TRA anomalous maps observed on Oct 19th, 2011, 4 days in advance. Epicenter is marked with red star, tectonic plate boundaries with red line, and major faults with brown color (top, right) .C Yearly time series of night time OLR over the epicentral area, anomalous values (red), 2011 mean value OLR (gray), 2006-2011 mean value (black), 2010 anomalous trend (blue) with no major seismicity for comparison. D. 2011 seismicity (EMSC catalog) M>4 near the epicentral area (bottom, black)*

The continuous satellite monitoring of OLR data over Greece obtained from NOAA POES satellite system showed rapid increase during the middle of April 2015 and they indicated a probable large earthquake preparation process in Aegean Sea (Fig. 4). A strong anomaly in the atmosphere was detected (prospectively) at 19:00 LT on May 14, 2015 with 2.5 sigma significance over 25 years of data analysis (Ouzounov et al, 2015). On May 24, 2015, after the anomaly was detected a M6.9 earthquake occurred in the area of the observed atmospheric anomaly.

*Figure 4. TRA associated with M6.9, May 24, 2014, earthquake in the Aegean Sea. A/.USGS shake map (top left),  B. Nighttime TRA anomaly map observed on May 14, 2015, 10 days in advance. Epicenter is marked with red star, tectonic plate boundaries with red line, and major faults with brown color (top, right) .C Yearly time series of night time OLR over the epicentral area, anomalous values (red), 2014 mean value OLR (gray), 2006-2041 mean value (black), 2013 anomalous trend (blue) with no major seismicity for comparison D. Seismicity (EMSC) M>4 near the epicentral area (bottom, black).*

During end of July and firing the August 2014 we detected (prospectively) a large TRA anomaly transient field over Northern California (Fig. 5). The location was shifted north West by about 100 km from the M6.0 of Aug 24rd epicentral area. For this particular case we used a hybrid OLR product between NOAA AVHHR and EOS AIRS observations to advance the temporal coverage of the San Francisco area. In the Southern Napa Valley, California earthquake the value of the OLR compared to the reference field of August 2004 to 2014, indicated a rapid change in the thermals anomalous flux rate at 7:00 on August 23. The registered anomalous pattern was the largest energy flux anomaly over the California at this time. (Ouzounov et al., 2014)
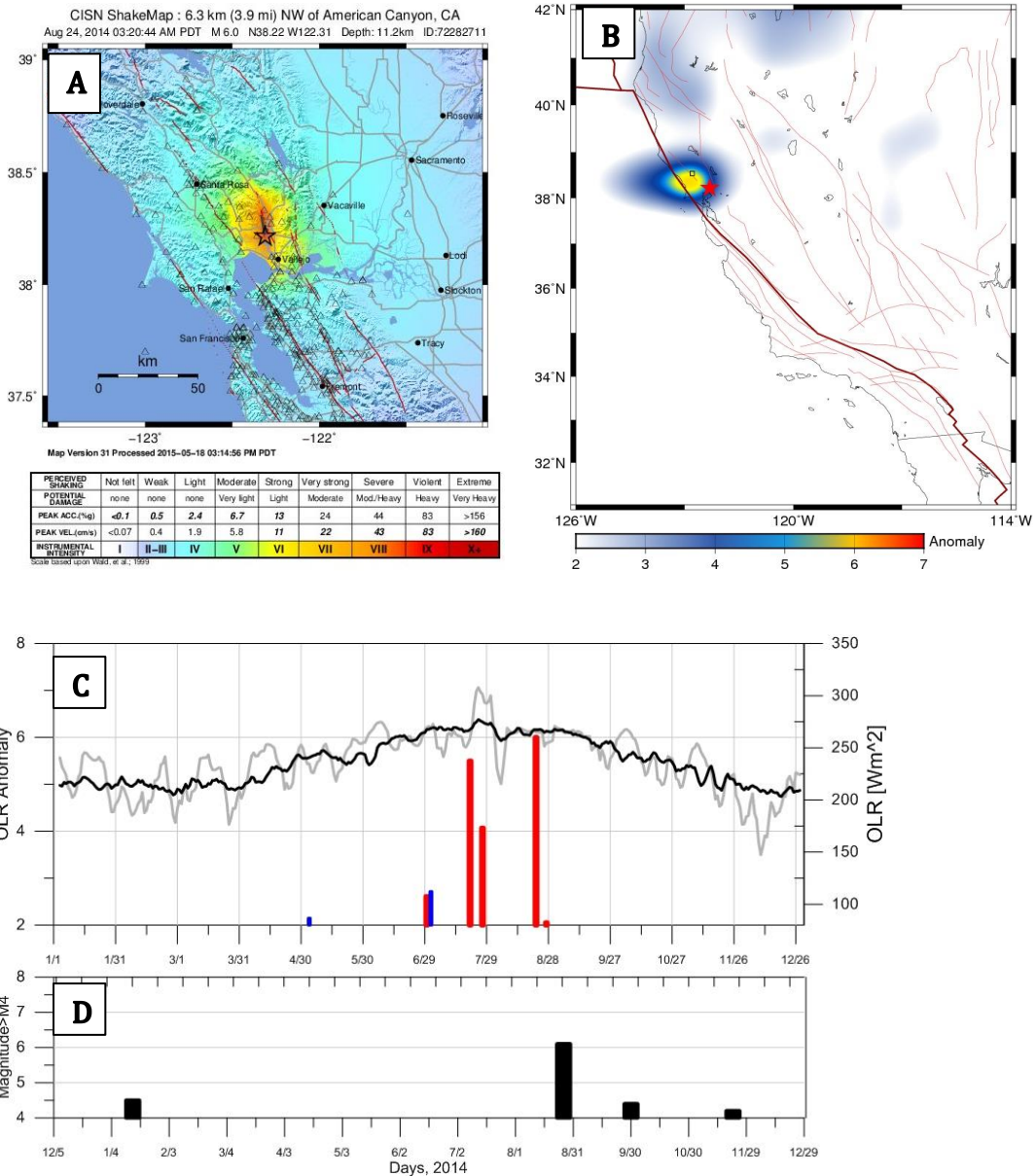
*Figure 5. TRA associated with M6 Aug 24, 2014, Napa Valley, California; A/.USGS shake map (top left), B. Nighttime TRA anomaly map observed on Aug 22nd 2014, 2 days in advance. Epicenter is marked with red star, tectonic plate boundaries with red line, and major faults with brown color (top, right) .C Yearly time series of night time OLR over the epicentral area: anomalous values (red), 2014 mean value OLR (gray), 2006-2014 mean value (black), 2013 anomalous trend (blue) with no major seismicity for comparison. D. 2014 seismicity (EMSC) M>4 near the epicentral area (bottom, black)*

The daily OLR variations (OLR anomalous values <=2) are caused by the daily environmental variations in the vertical atmospheric circulations in middle atmosphere. The significant deviation from the normal state for Van case started September 15, reached a maximum value (OLR,7) on October 22 and went back to normal state n December 15, 2011 (Fig.3) . For 2014 Aegean Sea event the breakout started in the beginning of February, the anomaly reached a maximum around May14 and came back to normal on October 15, 2014 (Fig.5) . For South Napa the break started in July 20 with a systematic increase reaching the maximum level (OLR values are around 7) in the OLR acceleration on August 22 and going back the normal state in mid-September 2014 (Fig.5).

At the ending of the event the anomalous pattern coincided with the same period as the ending of the major aftershock activities in all of the cases. To test the significance of the results for confutation – i.e. absence of anomalous OLR signals in absence of major

seismic events (Tramutoli et al, 2005), we calculated the OLR anomalies for the same location for one full year before the major event. The yearly time distribution of OLR shows significant lower level (Fig, 3,4, and 5 with blue columns) with a randomly distributed pattern. Thus it is not reproducing the strength and temporal evolution of the OLR anomalous signals generated during the year (Fig, 3,4,and 5 with red columns). The pre-earthquake OLR anomalies for M7.0 Van (Fig. 3) and M6.9 Greece (Fig .4 ) are not overlapping in time with the maxima of the  seasonal variations  of OLR usually higher during June-August in the Northern Hemisphere (Fig 3.4, black color curve), which is an indication for the non-weather related origin of OLR anomalous values and their primarily connection with the geodynamics. The M6.0 South Napa occurred in the middle of the summer, 2014 (August 24) and shows that the computational approach used can  rival an anomalous pattern even during a period of natural enchantment of the background radiation field (Fig 5). Analogous findings were observed within a few days prior to the most recent major earthquakes in Japan (M9, Tohoku, 2011), China (M7.9, Wenchuan 2008), Italy (M6.3, L'Aquila 2009), Samoa (M7, 2009), Haiti (M7, 2010) and Chile (M8.8, 2015) (Ouzounov et al., 2015ab; Pulinets et al., 2015).

**3. Thermal energy associated with some large earthquakes**

We have examined the different energy components of recent strong earthquakes (M>8), using observations and theory. Our motivation is to explore the physics of the associated thermal phenomena, *i.e*. to compare the energy of the earthquakes, as well as the latent heat released prior to the events. We have examined the energy budget of earthquakes via theory and observations for the three mega quakes of Sumatra, M9.1, 26 December 2004; M8.7, 28 March 2005; and M9.0, Tohoku, 2011 and evaluated mechanical and thermal energies. In other words, we evaluated the thermal energy, required to create the energy budget associated with these large quakes (Pulinets et al., 2006a, 2006b, Kafatos et al., 2010). Space-based observations and model outputs can be used for pre-seismic energy. We expect that our analysis will shed light on underlying physics (such as of our proposed pre-earthquake lithosphere/ atmosphere/ interaction) associated with some of the largest earthquakes and would potentially be useful for warning of future events. It is large events that give us information about the total energetics and, therefore, they are very useful to provide information about the underlying physics.

For the seismic moment $M_o$, one can use the rupture length, the rupture width and the slip to obtain values of 8.9 x $10^{22}$ J, 1 x $10^{22}$ J and 3.2 x $10^{22}$ J for the 26 Dec. 2004, the 28 March 2005, and 11 March 2011 events, respectively. We calculated that 2,000 $km^3$ land mass was displaced in the 26 Dec. 2004 Sumatra earthquake, while 1,300 $km^3$ of land mass was displaced in Japan. The seismic moment can be considered to be the total energy in the pre-quake stressed configuration, and is essentially an estimate of the total available energy budget. It is also close to estimate of change in gravitational potential energy Mgh, where M is the mass of the plate, g is gravitational acceleration, and h is the vertical distance the plate is displaced. The original Richter energy was supposed to refer to local damage near the epicenter. But the available energies are much higher than energies creating havoc at the surface. We are estimating the energies of seismic moment, latent heat and moving of landmasses. It is not surprising then that mega quakes of magnitude 9 seem to affect the entire Earth. We can estimate the change in the rotational energy of the Earth for these large events as, for example, the rotational rotation period of the Earth decreased 2.68 microseconds while the oblateness decreased by 1 part in $10^{10}$ for the main Sumatra event (Gretchen, 2005).

We compared the latent heat (LH) energy, obtained by integrating   (SLHF) over the area and the time of the earthquake, accounting for the overall thermal and mechanical associated energies. The SLHF data used are taken from NCEP/NCAR dataset maintained at the International Research Institute on Climate Prediction (IRI) (http://iri.columbia.edu). Thermal outgoing long wave radiation (OLR) data can also be used.

We compared the magnitudes of the energies associated with the 9.3, 8.7 and 9.0 events and their accompanying phenomena. Using the usual conversion of magnitudes to energy (Bath, 1996) associated with surface waves, $E_Q \sim 4.5 \times 10^{18}$ J , $E_Q \sim 5.5 \times 10^{17}$ J, and $1.5 \times 10^{18}$ J respectively. The total energy release of the entire series of earthquakes, including the many aftershocks, is dominated by these three events. The latent heat energy released prior to the earthquake, $E_{LH}$, can be estimated by:

$$\mathrm{D}SLHF(\mathbf{r}) = \sum_{i=1}^{N-1} \frac{SLHF(r)}{N-1}$$

(4)

where $\mathbf{r}$ is taken in practice by summing pixel by pixel ($\mathbf{r}$) and integrating over time. The result is insensitive because of the strongly peaked nature of the signal occurred around 7 Dec., 2004, 19 days in advance of the 26 December 2004, Sumatra earthquake (Cervone et al, 2004);  and similarly on March 3-10, associated with Tohoku earthquake (Ouzounov et al., 2011). The total LH associated with the three main events are $E_{LH} \sim 8.0 \times 10^{18}$ J, $3.1 \times 10^{19}$ J and $1.9 \times 10^{19}$ J associated the 28 March 2005 , 26 Dec. 2004 and 11 March 2011 earthquakes respectively, (See Table 2 ).

| | Events | $M_w$ | $E_Q$ Richter $x10^{17}$ J | Rupture length | LH energy $x10^{18}$ J | SLHF, $Wm^2$ | SLHF Durations |
|---|---|---|---|---|---|---|---|
| 1 | 12.26.2004, Sumatra | 9.1– 9.3 | 420 | ~1500km | ~310 | 100 | 10 days |
| 2 | 03. 28.2005, Sumatra | 8.7 | 5.7 | ~300km | ~8 | 80 | 5 days |
| 3 | 03.11. 2011, Japan | 9.0 | 150 | ~500km | ~190 | 90 | 8 days |

*Table 2 Energies comparison for the major earthquakes in Sumatra 2004, 2005 and Tohoku 2011,Japan*

The above energy values give us the main energy channels involved.. It would be important to research the interconnection between the mechanical processes and their energies, including the latent heat, and associated thermal energies (see below), which might be observed as surrogates for the total energies involved in earthquakes. The poorly resolved global energies may very well turn out to be the dominant term is the latent heat energy release, $> \sim 3 \times 10^{19}$ J, as we are observing LH, released through the ocean, while the mechanical/kinetic energies are an order of magnitude or less and the energy of rupture an order of magnitude higher.
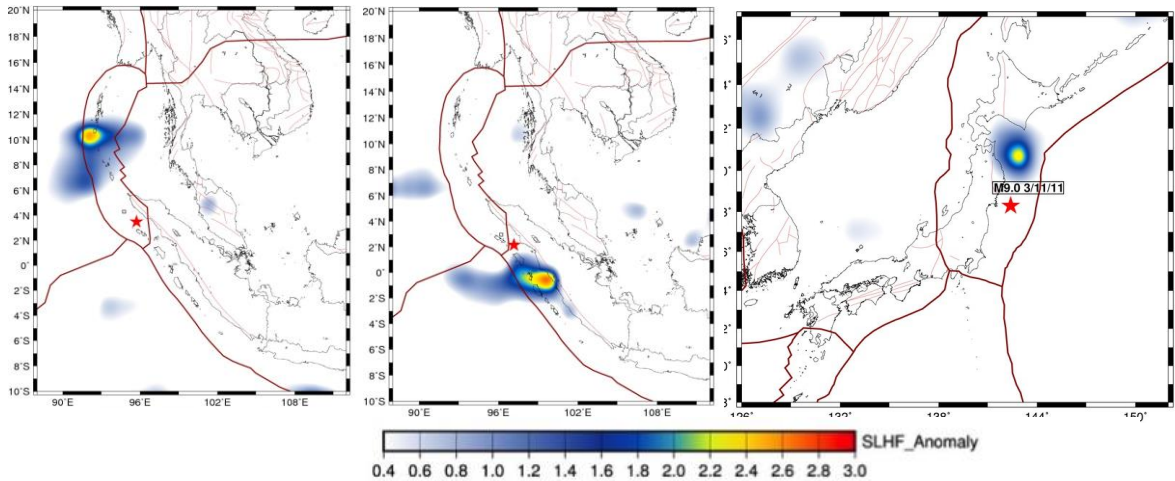
*Figure 6. Anomalous daily maps of SLHF a/. Dec 15, 21004, eleven days before M9.3 of Dec 26 Sumatra 2004; b/.March 6, 2005, twenty days before Sumatra 2005; c/March 5, 2011, six days before Tohoku 2011. Epicentres are marked with red star, tectonic plate boundaries with red line, and major faults with brown colour.*

Our analysis shows that latent heat has been detected several days prior to the earthquake. On Dec 15, 2004, eleven days before the M9.3 Sumatra earthquake a strong anomaly was observed along the rupture zone north of the site of the future epicenter, with a value >4 sigma (Fig, 6a). Similar phenomena with lower intensity and spatial extension were observed on March 6, 2005, twenty days before the March 26, 2005 M8.6 earthquake (Fig. 6b). For the 2011 Tohoku a similar pattern occurred, on March 5, only 6 days before the main shock, strong SLHF anomaly was observed north of the epicentral area, along the future rupture zone (Fig. 6c). As such, the overall earthquake phenomenon apparently causes LH release; suggesting that terrestrial internal energy is used to produce evaporation. The change in internal energy on a short timescale such as the December 2004, M9.3 earthquake in Sumatra, March 2005 for M8.6 and March2011 for M9.0 in Tohoku, We found that the ratios of the seismic moment; and the change of mechanical energy, to latent heat, is also a function of the size of the rupture, indicating latent heat is a direct surrogate of the total geophysical energies involved.

4. **Thermal anomalies and the Lithosphere-Atmosphere coupling**
Several processes have been considered as possible contributors to the transient short-lived ''thermal anomalies'': (a) rising fluids that would lead to the emanation of warm gases (Salman et al., 1992; Gorny et al., 1988); (b) rising well water levels and $CO_2$ spreading laterally and causing a ''local greenhouse'' effect (Qiang et al., 1991; Tronin et al., 2002; Tramutoli et al., 2005); (c) activating positive-hole pairs during rock deformation (Freund, 2002); (d) frictional heat around the active fault (Tagami et al., 2008); and (e) air ionization by radon and latent heat change due to change of air humidity (Pulinets and Ouzounov 2011).
TIR anomalies observed from satellites and associated with earthquake processes are less likely to be the result of: (i) earth crust heat flow (because of short-lived phenomena); (ii) convective transport as result of friction processes associated with active faulting (because of their rapid build- up); or (iii) meteorological origin (because of the long persistence of TIR over the same region). The most probable cause of the physical mechanism of the thermal anomaly generation can be the morphology and the release of thermal energy estimations. The most important one is that thermal anomalies are observed over both the land and the ocean. Only strong gas discharges (including the underwater gas discharges), as described by Khilyuk et al. (2000), could be a potential candidate for this possible mechanism.
Although their detailed underlying mechanisms are still under debate (*e.g.* Freund, 2011; Pulinets and Ouzounov, 2011), in the case of earthquakes, the general process that could affect the atmosphere and ionosphere "from below" might be the generation of TRA and the penetration of anomalous electric fields originating close to the surface extending into the ionosphere (Kuo et al., 2011). It was instrumentally documented that the latest stage of the earthquake cycle (Dobrovolsky *et al*., 1979) is characterized by mechanical changes in the Earth's crust accompanied by geochemical and electromagnetic anomalies (Scholz *et al*., 1973; Kasahara, 1981).The link between the crustal transformation under loading and asperities on faults has been studied (Schorlemmer et al., 2004). The formation of asperities, increasing crustal porosity this leads to changes in gas migration evidently by an increase of gas release into the boundary layer of the atmosphere.
At the last stage of earthquake preparation we observe the activation of faults within the

area of the earthquake within this area that leads to increased emanation of gases such as carbon dioxide, methane, hydrogen, helium, including radon (Step #1, Fig.7). It was established that together with radon diffusion within the crust it is actively released in the atmosphere by carrier gases, which usually are carbon dioxide and methane. A correlation was established between the deformations and radon release (Aumento, 2002). Radon, due to its radioactivity, produces the air ionization (Harrison et al., 2010) (Step #2, Fig.7).

Air ionization accelerates, drastically, the formation of cluster ions due to newly formed ion hydration. This process is called Ion Induced Nucleation (IIN) (Laakso et al., 2002). (Step #3, Fig.7).This process leads to formation of large charged ion clusters consisting of the charged core ion with the envelope of water molecules, which attach to the ions due their high dipole moment (Sekimoto and Takayama, 2007). IIN is essentially nonlinear process because it is catalytic exothermic process with simultaneously coexisting two aggregation phase states of the water: condensed and vapor.

We will discuss the key question in relationship between the generation of TRA in the atmosphere and the pre-earthquake process. The question is -*What are the drivers producing a strong modification of the atmosphere?* There is a paradox between the catalytic process: and the energy release, but the source of the energy is different. In the case of TRA it is the latent heat of the water vapor in the air. Here are some estimates:

The latent heat constant is $Q = 40.683$ kJ/mol, it means that the heat released per one molecule is $U0 = Q/NA = 0.422$ eV where $NA = 6.022 \cdot 10^{23}$ 1/mol (Avogadro number). Ionization effectiveness depends on the number of water molecules attached to the ion. If the particle grows to some value of $m_{max}$, the number of energy release will be: $w = m_{max}U0$. If the ion production rate is $dN/dt$, the heat released in the atmosphere could be expressed as $Pa = w \cdot dN/dt$. Experimentally the clusters of the order of 1000 nm were found (Pulinets and Ouzounov, 2011). To ionize any air molecules we need the energy of 10-15 eV. One particle of 1000 nm size contains $0.4 \cdot 10^{12}$ water molecules this produces the heat release 0.422 eV x $0.4 \cdot 10^{12} = 1.7 \cdot 10^{11}$ eV. So one can easily see that the energy gain due to the latent heat release is $1.7 \cdot 10^{11} /15 = \sim 10^{10}$. This is the essential value - *Radon and ionization does not produce any energy, the energy is released due to condensation of the water vapor on ions, and consequent release of the latent heat contained in the air water vapor*.
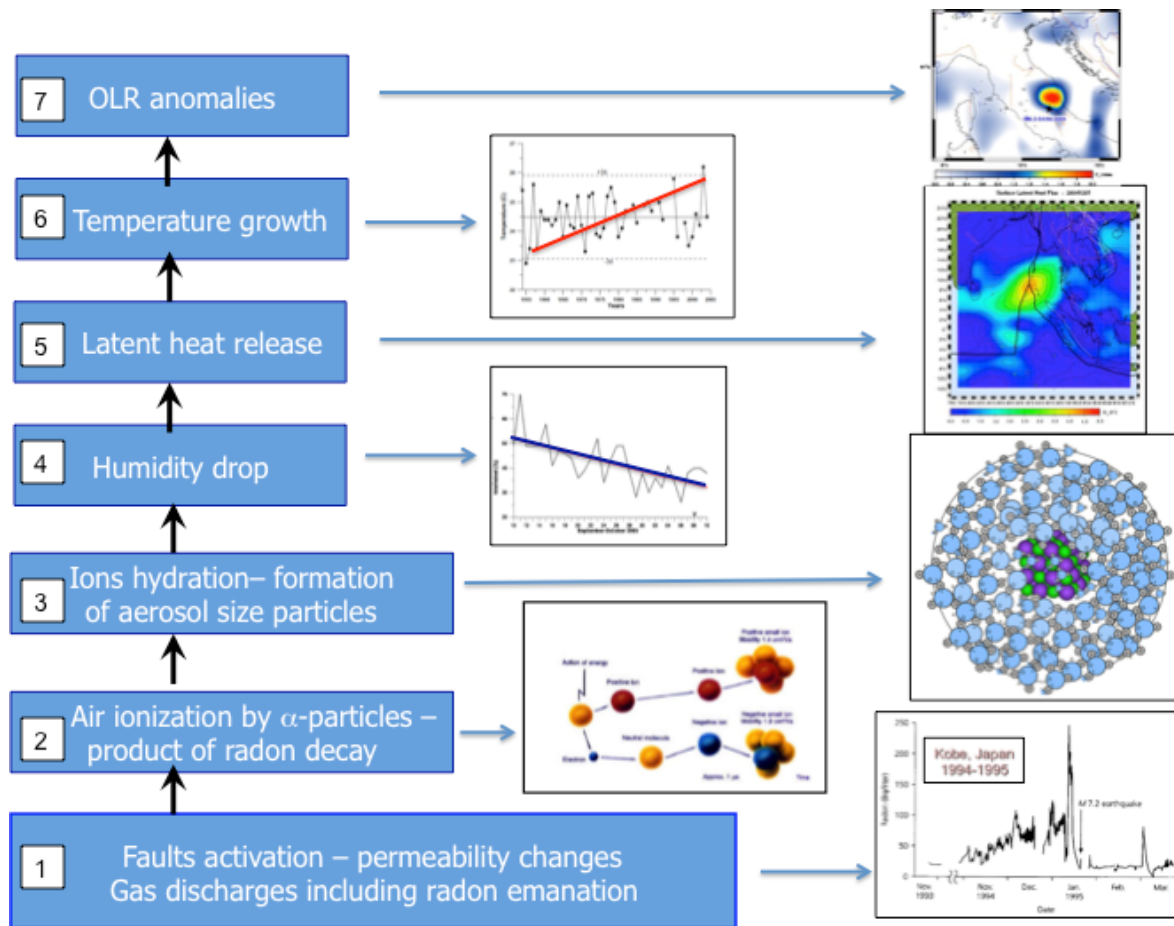
*Figure 7. Principle Flow-chart of the TRA generation (Pulinets and Ouzounov, 2011)*

In Fig.7 we can now explain rectangles Step #4 (relative air humidity drop because of water vapor condensations on ions), Step #5 (the latent heat release) and Step #6 (air temperature growth). It is well known from meteorology that sharp drops of humidity are accompanied by air temperature growth. Because of the general atmospheric circulation the additional heat flux release due to the latent heat release could be registered in the long wave part of the infrared emission within the transparency window of the atmosphere 8-12 μm from satellites (so called outgoing Longwave radiation – OLR), (step #7 Fig. 7). *What is amount of outgoing energy flux we should expect at TOA as Outgoing Longwave Radiation flux was shown in Fig. 1?* Each α-particle emitted by $^{222}$Rn with the average energy of E$\alpha$=5.46 MeV can produce ~ $3\cdot10^5$ electron-ion pairs. From the real observation of radon activity, before an earthquake the level could be ~2000 Bq/m$^3$ (Inan et al., 2008). The ion production rate of Rn is ~$6\cdot10^8$ s$^{-1}$. We already show from our last estimation that the particle 1000 nm size contains $0.4\cdot10^{12}$ water molecules. During the water vapor condensation process the latent heat release is $U_0 \sim 40.68\cdot10^3$ J/mol (1 mol = $6.022\cdot10^{23}$). That means that the given radon activity with formation of particles of 1000 nm size gives the thermal energy output of 16 W/m$^2$ . That is exactly the range of ~20W/m$^2$ we were able to observe as TRA anomalies at TOA by using NOAA/AVHRR data (Ouzounov et al, 2007). There are two main consequences of the IIN process: (1) latent heat release due to water vapor condensation on ions; and (2) changes of the air conductivity leading to the local changes in the Global Electric Circuit – for the electromagnetic coupling of the atmosphere and ionosphere. The chain of these physical processes has been proposed as an essential part of the Lithosphere-Atmosphere-Ionosphere-Magnetosphere Coupling concept. (Pulinets and Ouzounov, 2011, Pulinets et al., 2015). The presence of thermal infrared anomalies (TIR) at different levels (ground level, troposphere, tropopause) and space plasma anomalies including the GPS/TEC,

allow us to register them from space using a multi-parameter approach (Ouzounov et al, 2011)

## 5. Summary and Conclusions

Our results show that several days before some earthquakes (Figs. 3,4,5 ) infrared signals related to earthquake processes were observed near the epicentral areas by the NOAA POES satellite as OLR hotspots. The OLR hot spots appeared quickly, stayed over the same regions from several hours or up to few days, and then disappear rapidly. The time lag for the M7.3 earthquake in Van, Turkey was 4 days; for the M6.9 earthquakes in Aegean Sea, Greece was 10 day and for M6.0 earthquake in California was 2 days. This enhancement of OLR could be explained as a result of water vapor condensation on ions, with a large amount of latent heat being released. The initial process involves an ionization of the near-ground layer due to an increased concentration of gasses (including radon) emitted from active tectonic faults (Pulinets and Ouzounov, 2011). The transient nature in radiative emission preceding large earthquakes follows a general temporal-spatial evolution pattern, which is similar to other large earthquakes worldwide (Kuo, 2011 and Ouzounov et al., 2016). The transitional OLR anomalous data usually varied between 16-21 $W/m^2$. They are residuals derived from the daily mean OLR compared with the background field. The latter was derived from multiple years of observations, over the same location and local time, and normalized by the standard deviation (Ouzounov et al, 2007, 2011). From space-born observations of atmospheric conditions, we have shown the consistent occurrence of TRA anomalies at the TOA, over the region of maximum stress associated with, and preceding, large earthquakes. Because of their relatively long duration, these anomalies do not appear to be of meteorological origin. We evaluated the mechanical and thermal energies of three major earthquakes to explore the physics of associated thermal phenomena. Our estimates show that the LH released prior to the events is larger than the seismic energy released during the quake. We show that in large earthquakes the associated phenomena may stand out energetically with measurements above variance that arises from other geophysical processes. As we have a greater energy budget for these large events, we emphasize that it can be used to establish a more general earthquake energy phenomenology. Our analysis of transitional thermal fields of recent major earthquakes (M7.3 Van, Turkey, 2011; M6.9 Aegean sea, Greece, 2014; and M6.0 Napa Valley, California, 2014) has demonstrated the presence of correlated variations of TRA anomalies in the atmosphere, implying their connection with pre-earthquake processes. Our results suggest the existence of an atmospheric response triggered by the coupling processes between the lithosphere and atmosphere.

# Reference

Aumento, F. (2002), Radon tides on an active volcanic island: Terceira, Azores, Geofísica Internacional, 41,4,p. 499–505.

Bath, M., (1966), Body wave energy from seismograms. In:L.H. Ahrens et al. (Editors), Physics and Chemistry of the Earth. Pergamon Press, London, 7: 133-137.

Bryant, N., Zobrist, A., Logan, T., (2003), Automatic co-registration of space-based sensors for precision change detection and analysis. IGARSS 2003 Transactions. France, 7. 21–26

Carreno, E., Capote, R., Yague, A., (2001) Observations of thermal anomaly associated to seismic activity from remote sensing. General Assembly of European Seismology Commission, Portugal, 10–15 September, 265–269.

Cervone, G,Kafatos, M,Napoletani, D,Singh, RP, (2004) ,Wavelet maxima curves of surface latent heat flux associated with two recent Greek earthquakes, Natural Hazards and Earth System Sciences, VL 4,IS 3, 359-374

Cervone, G.,Maekawa, S., Singh, R.P., Hayakawa, M., Kafatos, M., and Shvets, A., (2006), Surface latent heat flux and nighttime LF anomalies prior to the Mw=8.3 Tokachi-Oki earthquake, Nat. Hazards Earth Syst.

Dey, S., Sarkar, S., Singh, R.P., (2004), Anomalous changes in column water vapor after Gujarat earthquake. Advances in Space Research33 (3), 274–278

Di Bello, G., Filizzola, C., Lacava, T., Marchese, F., Pergola, N., Pietrapertosa, C.,Piscitelli, S., Scaffidi, I., Tramutoli, V.(2004) Robust. satellite techniques for volcanic and seismic hazards monitoring. Annals Geophys. 47 (1), 49–64

Dobrovolsky, I. R., S. I. Zubkov, and V.I. Myachkin, (1979) ,Estimation of the size of earthquake preparation zones, Pageoph., 1025 -1044

Filizzola C., Pergola N., Pietrapertosa C., Tramutoli V. (2004), Robust satellite techniques for seismically active areas monitoring: a sensitivity analysis on September 7th 1999 Athens's earthquake. Physics and Chemistry of the Earth, 29, 517-527.

Fisher, S., K. Sulia, D. Ouzounov, F. Policelli, and M. Ferrucci (2008), Data Exploration of Atmospheric Thermal Signals over Regions of Tectonic Faulting and Earthquake Processes, AGU Fall Meeting Abstracts

Freund, F., (2002), Charge generation and propagation in rocks, J.Geodynamics 33, 545–572

Freund, F. (2011), Pre-earthquake signals: Underlying physical processes, J. of Asian Earth Sci., 41, 383–400

Genzano N., Aliano C., Filizzola C., Pergola N., Tramutoli V. (2007), A robust satellite technique for monitoring seismically active areas: the case of Bhuj - Gujarat earthquake. *Tectonophysics*, 431, 197-210

Genzano, N., Aliano, C., Corrado, R., Filizzola, C., Lisi, M., Mazzeo, G., Paciello, R., Pergola, N., Tramutoli, V. (2009), RST analysis of MSG-SEVIRI TIR radiances at the time of the Abruzzo April 6th 2009 earthquake. *Natural Hazards and Earth System Sciences* - vol. 9, pp. 2073-2084.

Goosse H., P.Y. Barriat, W. Lefebvre, M.F. Loutre and V. Zunz, (2016). Introduction to climate dynamics and climate modeling. Online textbook available at http://www.elic.ucl.ac.be/textbook.

Gorny, V.I., Salman, A.G., Tronin, A.A., Shilin, B.B., (1988), The Earth outgoing IR radiation as an indicator of seismic activity. Proceeding of the Academy of Sciences of the USSR, 301: 67.

Gretchen Cook-Anderson, Dolores Beasley, (2005) NASA Details Earthquake Effects on the Earth. *NASA* (press release). *January 10, 2005*

Gruber, A. and Krueger, A., (1984), The status of the NOAA outgoing longwave radiation dataset. Bulletin of the American Meteorological Society ,65, 958–962

Han, P., Hattori, K., Hirokawa, M., Zhuang, J., Chen, C.H., Febriani, F., Yamaguchi, H.,

Yoshino, C., Liu, J.Y., Yoshida, S., (2014) Statistical analysis of ULF seismomagnetic phenomena at Kakioka, Japan, during 2001-2010. Journal of Geophysical Research: Space Physics 119, 4998–5011.

Han, P., Hattori, K., Huang, Q., Hirooka, S., Yoshino, C., (2016) Spatiotemporal characteristics of the geomagnetic diurnal variation anomalies prior to the 2011 Tohoku earthquake (Mw 9.0) and the possible coupling of multiple pre-earthquake phenomena. Journal of Asian Earth Sciences 129, 13–21.

Hayakawa, M. (1999), *Atmospheric and Ionospheric Electromagnetic Phenomena with Earthquakes*, Terra Sci. Pub. Co., Tokyo.

Hayakawa, M. and O. A. Molchanov (2002), *Seismo Electromagnetics, Lithospheric-Atmospheric- Ionospheric coupling*, Terra Sci. Pub. Co., Tokyo.

Hayakawa, M (Editor), (2012), Frontier of Earthquake short-term prediction study, Nihon-Senmontosho, Japan, 794p

Harrison R.G., Aplin K.L., Rycroft M.J. (2010) Atmospheric electricity coupling between earthquake regions and the ionosphere, JASTP, 72, 376–381, 2010

Inan S, Akgu T, Seyis C, Saatc R, Baykut S, Ergintav S and Bas M (2008). Geochemical monitoring in the Marmara region (NW Turkey): A search for precursors of seismic activity. *J Geophys Res* **113**: B03401, doi:10.1029/2007JB005206.

Kafatos, M., D. Ouzounov, S. Pulinets, K. Hattori, J. Liu, M. Parrot, and P. Taylor , (2010), Multi Sensor Approach of Validating Atmospheric Signals Associated with Major Earthquakes, EGU General Assembly Conference Abstracts 12, 1418

Kasahara, K., (1981) Earthquake Mechanics, Cambridge University Press, Cambridge, 1-248,

Kuo, C.L., Huba, J.D., Joyce, G., Lee, L.C. (2011) Ionosphere plasma bubbles and density variations induced by pre-earthquake rock currents and associated surface charges. Journal of Geophysical Research, 116, 1029-1039

Kon, S., M. Nishihashi, and K. Hattori (2010), Ionospheric anomalies possibly associated with M ≥ 6 earthquakes in Japan during 1998-2010: Case studies and statistical study, *J. Asian Earth Sci.*, **41(4)**:410-420, DOI: 10.1016/j.jseaes.2010.10.005

Laakso L, Mäkelä JM, Pirjola L, Kulmala M (2002), Model studies on ion-induced nucleation in the atmosphere. J. Geophys. Res., 107(D20): 4427, doi:10.1029/2002JD002140

Liebmann B. and C.A. Smith, (1996), Description of a Complete (Interpolated) Outgoing Longwave Radiation Dataset. Bulletin of the American Meteorological Society, 77, 1275-1277.

Lisi M., Filizzola C., Genzano N., Grimaldi C. S. L., Lacava T., Marchese F., Mazzeo G., Pergola N. and Tramutoli V (2010) A study on the Abruzzo 6 April 2009 earthquake by applying the RST approach to 15 years of AVHRR TIR observations. Natural Hazards and Earth System Sciences, 10, pp. 395–406.

Liu, D., Kang, C., (1999) Thermal omens before earthquakes. ACTA Seismological Sinica 12 (6), 710–715

Liu, J. Y., Y. I. Chen, S. A. Pulinets, Y. B Tsai, and Y. J. Chuo, (2000) Seismo-ionospheric signatures prior to M>6.0 Taiwan earthquakes, Geophys. Res. Lett., 27, 3113-3116, 2000.

Liu, J. Y., Y. I. Chen, C. H. Chen, and K. Hattori (2010), Temporal and spatial precursors in the ionospheric global positioning system (GNSS GPS) total electron content observed before the 26 December 2004 M9.3 Sumatra-Andaman Earthquake, J. Geophys. Res., 115, A09312, doi:10.1029/ 2010JA015313.

MacArthur, Steven D (1980) Human spirit in Pauline usage. PhD thesis, University of Glasgow

Martinelli G, (1998), History of earthquake prediction researches, Il NuovoCimento C 22(3)

Mehta, A., and J. Susskind,(1999),Outgoing Longwavelength Radiation from the TOVS Pathfinder Path A Data Set, J.Geophys. Res., 104, NO.d10,12193-12212.

Milne J. (1913) Earthquakes and other movements, 2nd edition, London, 210p

Ohring, G. and Gruber, A.: (1982), Satellite radiation observations and climate theory, Advance in Geophysics., 25, 237–304, 1982.

Ouzounov, D., and F. Freund, (2004) Mid-infrared emission prior to strong earthquakes analyzed by remote sensing data, Adv. Space Res., 33(3), 268-273

Ouzounov D., Liu, D., Kang,C. , Cervone, G., Kafatos, M., Taylor, P. (2007), Outgoing Long Wave Radiation Variability from IR Satellite Data Prior to Major Earthquakes, Tectonophysics, 431, 211-220

Ouzounov D. S.Pulinets, K.Hattori, M, Kafatos, P.Taylor (2011), Atmospheric Signals Associated with Major Earthquakes. A Multi-Sensor Approach, in the book "Frontier of Earthquake short-term prediction study", M Hayakawa, (Ed), Japan, 510-531

Ouzounov D, S. Pulinets, J. Y. Liu, K. Hattori, P. Kalenda, W. Shen, V. S. Bobrovskiy,C. Windsor, M. Kafatos, and P.Taylor (2011), Utilizing new methodologies to study major earthquakes: Multi-parameter observation of pre-earthquake signals from ground and space, AGU Meeting Abstracts

Ouzounov, D., M. Kafatos, L. Petrov, S. A. Pulinets, J. Y. Liu, Y. C. Su, and S. Chen (2014), Space and Ground observations of Pre-earthquake Anomalies. Prospective/Retrospective Testing for M6.0 August 24, 2014 South Napa, CA, AGU Fall Meeting Abstracts 4942

Ouzounov, D., S. Pulinets, and D. Davidenko (2015a), Revealing pre- earthquake signatures in atmosphere and ionosphere associated with 2015 M7.8 and M7.3 events in Nepal. Preliminary results, arXiv:1508.01805

Ouzounov D, S. Pulinets, K.Hattori, L.Lee, J.Y.Liu and M.C. Kafatos (2015b), Prospective Validation of Pre-earthquake Atmospheric Signals and Their Potential for Short–term Earthquake Forecasting Geophysical Research Abstracts Vol. 17, EGU2015-7840-1, EGU General Assembly

Ouzounov D, S.Pulinets, D. Davidenko, M.Hernández-Pajares , A.García-Rigo , L. Petrrov, N. Hatzopoulos , M. Kafatos (2016), Pre–earthquake signatures in atmosphere /ionosphere and their potential for short-term earthquake forecasting. Case studies for 2015, Geophysical Research Abstracts, Vol. 18, EGU2016-3496, EGU Assembly

Pergola N., Aliano C., Coviello I., Filizzola C., Genzano N., Lacava T., Lisi M., Mazzeo G. and Tramutoli V. (2010) Using RST approach and EOS-MODIS radiances for monitoring seismically active regions: a study on the 6 April 2009 Abruzzo earthquake. Natural Hazards and Earth System Sciences, 10, pp.239–249

Pulinets S, and K. Boyarchuk (2014) *Ionospheric Precursors of Earthquakes*, Springer,

Pulinets S, Ouzounov, D Ciraolo L.; Singh, R.; Cervone, G.; Leyva, A.; Dunajecka, M.; Karelin, A.V.; Boyarchuk, K.A.; Kotsarenko, A. (2006a) ,Thermal, atmospheric and ionospheric anomalies around the time of the Colima M7.8 earthquake of 21 January 2003. Ann. Geophys. 2006, 24, 835-849.

Pulinets S, Ouzounov D, Karelin A, Boyarchuk K, Pokhmelnykh L,(2006b), The physical nature of thermal anomalies observed before strong earthquakes, Physics and Chemistry of the Earth, Volume 31, Issue 4-9, p. 143-153

Pulinets S and D Ouzounov, (2011), Lithosphere–Atmosphere–Ionosphere Coupling (LAIC) model–An unified concept for earthquake precursors validation, Journal of Asian Earth Sciences 41 (4), 371-382

Pulinets, S., and Davidenko, D ,(2014), Ionospheric precursors of earthquakes and global electric circuit, Adv. Space Res., 53(5), 709-723

Pulinets S., D. Ouzounov, A.Karelin, D. Davidenko (2015) Physical Bases of the Generation of Short-Term Earthquake Precursors: A Complex Model of Ionization-Induced Geophysical Processes in the Lithosphere–Atmosphere–Ionosphere–Magnetosphere System, Geomagnetism and Aeronomy, 55, No.4, 540-558

Quing, Zu-Ji, Xu, Xiu-Deng, Dian, Chang-Gong. (1991) Thermal infrared anomaly - precursor of impending earthquakes. *Chinese science bulletin,* 36: 319

Salman, A., Egan, W.G., Tronin, A.A., (1992) Infrared remote sensing of seismic disturbances. In: Polarization and Remote Sensing. SPIE, San Diego, CA, pp. 208–218 (4), 319–323

Saraf, A, Choudhury, S.,(2005) NOAA-AVHRR detects thermal anomaly associated with 26 January,2001 Bhuj Earthquake, Gujarat, India. Int. J. Remote Sens, 26, 1065-1073

Schorlemmer D., Wiemer S., Wyss M., (2004), Earthquake statistics at Parkfield: 1. Stationarity of b-values, Journal of Geophysical Research*, 109, B12307, doi:*10.1029/2004JB003234

Scholz C.H., Sykes L.R., Aggarwal Y.P. (1973), Earthquake prediction: A physical basis, Science, 181, 803-809

Sekimoto, K., Takayama, M.(2007), Influence of needle voltage on the formation of negative core ions using atmospheric pressure corona discharge in air , International Journal of Mass Spectrometry, 261. p. 38–44

Susskind, J., and J. Blaisdell, (2008), Improved surface parameter retrievals using AIRS/AMSU data, Proc. SPIE Int. Soc. Opt. Eng., 6966, 696610, doi:10.1117/12.774759.

Tagami, T., Hasebe, N., Kamohara, H., Takemura K., (2008), Thermal anomaly around the Nojima Fault as detected by fission-track analysis of Ogura 500 m borehole samples. *Island Arc*, 10: 457

Tramutoli, V., Cuomo, V., Filizzola, C., Pergola, N., Pietrapertosa, C., (1999), Assessing the potential of thermal infrared satellite surveys for monitoring seismically active areas. The case of Kocaeli (İzmit) earthquake, August 17th, 1999, Remote Sensing of Environment, 96 (3-4), 409-426, 2005.

Tramutoli, V., Di Bello, G., Pergola, N., and Piscitelli, S., (2001), Robust satellite techniques for remote sensing of seismically active areas, Ann. Geophys., 44(2), 295-312, 2001.

Tramutoli, V., Aliano, C., Corrado, R., Filizzola, C., Genzano, N., Lisi, M., Martinelli, G., Pergola, N. , (2013), On the possible origin of Thermal Infrared Radiation (TIR) anomalies in earthquake-prone areas observed using Robust Satellite Techniques (RST). Chemical Geology, vol. 339, 157-168

Tramutoli V, Armandi B, Corrado R, Filizzola C, Genzano N, Lisi M, Paciello R, Pergola N , (2014a), Long term TIR satellite monitoring over Europe, Us and Asian regions: results and possible implications for an integrated system for a Time-Dependent Assessment of Seismic Hazard (T-DASH). In 2014 URSI GASS 2014 XXXIth URSI General Assembly And Scientific Symposium 1–2. 16-23 Agosto 2014, Beijing. Doi: 10.1109/URSI GASS.2014.6929870.

Tramutoli V, Armandi B, Coviello I, Eleftheriou A, Filizzola C, Genzano N, Lacava T, Lisi M, Paciello R, Pergola N, Satriano V, Vallianatos F, (2014b). Long Term RST Analyses of TIR Satellite Radiances in Different Geotectonic Contexts: Results and Implications for a Time Dependent Assessment of Seismic Hazard (t-DASH). American Geophysical Union (AGU) Fall Meeting 15-19 dicembre 2014 San Francisco

Tramutoli V., Corrado R., Filizzola C., Genzano N., Lisi M. and Pergola N. (2015a). From visual comparison to robust satellite techniques: 30 years of thermal

933    infrared satellite data analyses for the study of earthquake preparation phases.
934    Boll. Geof. Teor. Appl., 56 (2), 167-202,
935 Tramutoli V., Corrado R., Filizzola C., Genzano N., Lisi M., Paciello R. and Pergola N.
936    (2015b).  One year of RST based satellite thermal monitoring over two Italian
937    seismic areas. Boll. Geof. Teor. Appl., 56 (2), 275-294
938 Tributsch (1978) Do aerosols anomalies precede earthquakes? Nature, 276,1978,606-607
939 Tronin, A.A.(1996),  Satellite thermal survey—a new tool for the studies of seismoactive
940    regions. Int. J.Remote Sens. 1996, 17, 1439-1455.
941 Tronin, A.A.; Hayakawa, M.; Molchanov, O.A. (2002),   Thermal IR satellite data
942    application for earthquake research in Japan and China. J. Geodynamics, 33,
943    519-534.
944 Tronin, A.A.; Biagi, P.F.; Molchanov, O.A.; Khatkevich, Y.M.; Gordeeev, E.I., (2004),
945    Temperature variations related to earthquakes from simultaneous observation at
946    the ground stations and by satellites in Kamchatka area. Phys. Chem. Earth
947    2004, 29, 501-506
948 Tronin, A.A. ,(2006), Remote sensing and earthquakes: a review. Phys. Chem. Earth, 31,
949    138-142
950 Tronin, AA. (2011) Catalog of thermal and atmospheric phenomena associated with
951    earthquakes, Sankt Petersburg, Russia, (in Russian), 260pp
952
953